27/3-13-85 WB (1)

I-19744

DR-0839-7

UCID-18987-85

REPORT TO THE DOE NUCLEAR DATA COMMITTEE 1985

R. M. White
E-Division

and

R. G. Lanier
Nuclear Chemistry Division

February, 1985

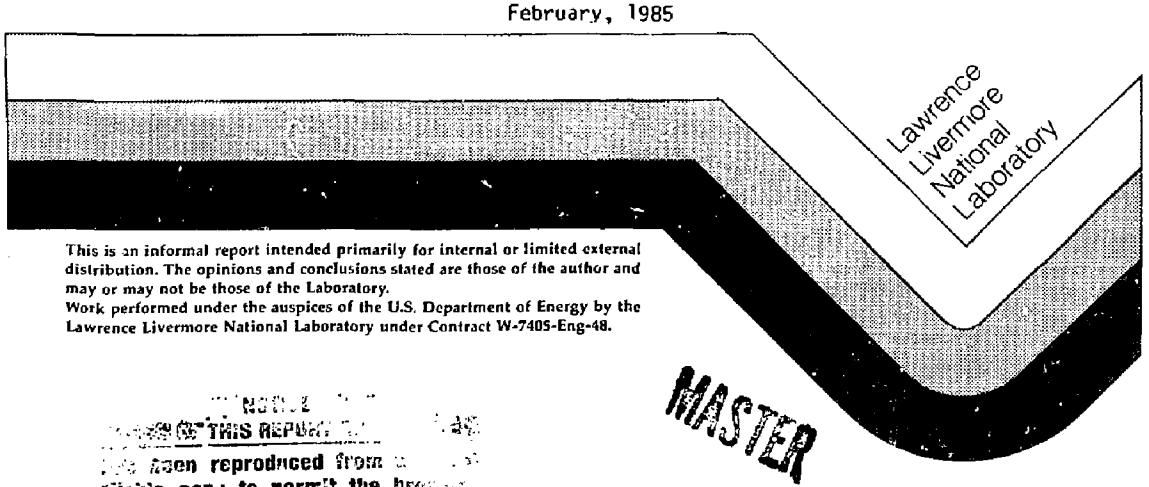

UCID--18987-85

DE85 008030

LAWRENCE LIVERMORE NATIONAL LABORATORY

A. NUCLEAR DATA APPLICATIONS-MEASUREMENTS

1. Measurements and Calculations of the Leakage Multiplication from Hollow Beryllium Spheres (Wong, Plechaty, Bauer, Haight, Hansen, Howerton, Komoto, Lee, Perkins, and Pohl)

Proposed fusion reactors utilize Be in the surrounding blanket to multiply the fusion neutrons for use in breeding tritium and in some cases also fissile material. To have confidence that the breeding is calculated correctly, it is essential to validate the Be cross sections via integral experiments. Recent measurements of the leakage multiplication from Be[1] and BeO[2] were 20 to 30% lower than calculations. The leakage multiplication is defined as the number of neutrons leaking out of the Be per 14-MeV source neutron introduced at its center. In view of the large discrepancies observed we have undertaken a program to calculate and measure the leakage multiplication from spherical Be shells as a function of thickness.

The method utilized is that of "Pulsed Spheres".[3] The Be spherical shells are pulsed at their centers with 14-MeV neutrons. These neutrons propagate outward through the spherical shells and are measured by time-of-flight techniques with NE213, Stilbene, and ^{6}Li glass scintillators positioned at 7.28 meters. We have measured the leakage spectra of high energy neutrons (> 1 MeV) with NE213 and Stilbene from spherical shells of Be of thicknesses 4.5, 14.2 and 19.9 cms. In all cases, the inner void radius was 8 cm. These Be thicknesses correspond to 0.8, 2.5, and 3.5 MFP (mean-free-path) for 14 MeV neutrons. Comparison with calculations employing ENDL-84[4] shows that excellent agreement is obtained for the leakage spectra above I-MeV neutron energy. Table A-1 presents the measured and calculated integrals of the leakage spectra for the 3.5 MFP Be shell. The agreement using ENDL-84 cross sections is within the estimated accuracy of the measurements, typically ± 5%. Similar agreement is observed for the smaller spherical shells.

---

1 T. K. Basu et al., Nucl. Sci. & Eng., 70, 309 (1979).

2 V. R. Nargundkar et al., Fusion Technology, 6, 93 (1984).

3 C. Wong et al., UCRL-51144, Rev.I, Lawrence Livermore National Laboratory (1972).

4 S. T. Perkins et al., UCRL-91276, Lawrence Livermore National Laboratory (1984).

TABLE A-1. Measured and Calculated Integrals (using ENDL-84) for 3.5 MFP Be (in terms of the ratio of detector counts with shell in divided by detector counts with shell out).

	Stilbene		NE213	
	Calc.	Meas.	Calc.	Meas.
$1.0 \leq E_n \leq 15$ (MeV)	0.600	0.574	0.658	0.653
$3.75 \leq E_n \leq 15$ (MeV)	0.351	0.349	0.371	0.369

Monte-Carlo calculations showed that, for the thickest Be shell, up to 40% of the leakage neutrons were below 1 eV. For the low energy measurements with ^{6}Li glass, helium bags were inserted in the flight path to reduce the attenuation of thermal and epithermal neutrons. The pulse repetition rate was decreased to 100 Hertz because the flight time of a thermal neutron is 3 ms. Figure A-1 shows the measured and calculated time-of-arrival spectra for the 3.5 MFP Be shell. Measurements extended out to 9 ms and the burst width was 10 μs. Calculations employed ENDL-84 Be cross sections. Figure A-1 confirms the predicted copious emission of epithermal and thermal neutrons from the large Be shell. A comparison of the calculated and measured integrals of the spectra in Fig. A-1 shows that ENDL-84 overestimates the total measured counts by 15% between thermal and ~2 MeV. The corresponding value for the 2.5 MFP Be shell is 5%. Folding in the results of the comparisons above 1 MeV, and estimating the accuracy of the detector efficiencies, we tentatively conclude that ENDL-84 overestimates the leakage multiplication by 13% for the 3.5 MFP Be, and by 5% for the 2.5 MFP Be.

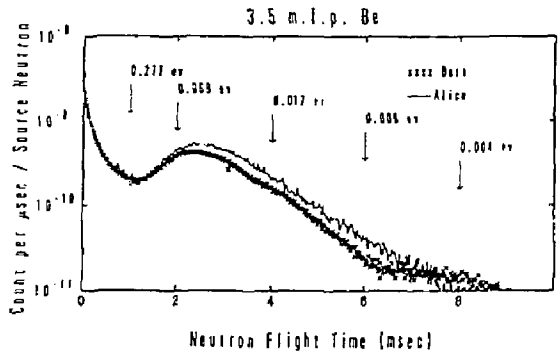

Fig. A-1. Measured and calculated time-of-arrival spectra for the 3.5 MFP Be shell.

2. Measurements of ^{6}Li and ^{7}Li Neutron-Induced Tritium Production Cross Sections at 15 MeV (Goldberg, Barber, Barry, Bonner, Fontanilla, Griffith, Haight, Nethaway, and Hudson)

Tritium production cross sections have been inferred from direct measurements of tritium generated in wafers of ^{6}LiH and ^{7}LiH under bombardment by 15 MeV neutrons produced at the Lawrence Livermore National Laboratory's RTNS-I facility. Sealed in a thin-walled Pb container, each hydride wafer was immersed in boiling Hg which first amalgamated the Pb and then dissociated the LiH. The hydrogen, acting as a carrier, was directed to an electronic counter and mixed carefully with methane. The counting procedure provided an accurate measure of tritium originally generated in each wafer. The TART Monte Carlo code was employed in the analysis of the data. The tritium production cross section for ^{6}Li exposed to 14.92 MeV neutrons is 32 ± 4 mb and that for ^{7}Li exposed to 14.94 MeV neutrons is 302 ± 15 mb.

3. Measurement of Fast Neutron Fission Yields (Nethaway, Momyer)

We irradiated ^{235}U, ^{238}U, and ^{239}Pu metal targets with fast neutrons from the FLATTOP Critical Assembly at the Los Alamos National Laboratory. FLATTOP is a natural-uranium-reflected ^{235}U or ^{239}Pu critical assembly which provides a neutron energy distribution in the central irradiation position which is slightly degraded from a pure fission-spectrum distribution. The uranium targets were irradiated in an oralloy core in FLATTOP, and the plutonium target in a plutonium core. The isotopic compositions of targets and cores were: ^{235}U (1.0% ^{234}U, 93.2% ^{235}U, 0.6% ^{236}U, and 5.2% ^{238}U), ^{238}U (0.18% ^{235}U and 99.82% ^{238}U), and ^{239}Pu (93.6% ^{239}Pu, 5.8% ^{240}Pu, and 0.6% ^{241}Pu). The targets weighed about four grams each, and were irradiated for four hours.

After the irradiations the target materials, which remained sealed in aluminum cans, were dissolved in closed systems so that the gaseous fission products could be collected for krypton and xenon analysis. Aliquots of the target solutions were taken for direct gamma-ray assay and for various chemical separations (rare-earths, cadmium, and antimony). The fission yields were measured relative to the yields of several well-known fission products (^{95}Zr, ^{99}Mo, ^{140}Ba, ^{144}Ce, and ^{147}Md).[5,6] Some of the measured fission yields are given in Table A-2. The yields have not been corrected for the isotopic impurities in the ^{235}U and ^{239}Pu targets.

---

[5] B. F. Rider, General Electric Co. Report, NEDO-12154-3(C), October (1981).

[6] D. R. Nethaway and G. W. Barton, Lawrence Livermore National Laboratory, UCRL-51458 (1973).

TABLE A-2. Fission yields measured for fast-neutron fission of ^{235}U, ^{238}U, and ^{239}Pu. The errors given do not include an uncertainty of about 3% in the number of fissions, or the uncertainty in the decay scheme.

	Fission Yield (atoms/fission)		
Nuclide	^{235}U	^{238}U	^{239}Pu
^{85}Kr	$(3.19 \pm 0.03) \times 10^{-3}$	$(1.66 \pm 0.04) \times 10^{-3}$	$(1.48 \pm 0.02) \times 10^{-3}$
$^{115}Cd^{g}$	$(3.19 \pm 0.06) \times 10^{-4}$	$(3.16 \pm 0.19) \times 10^{-4}$	$(6.76 \pm 0.17) \times 10^{-4}$
^{155}Eu	$(4.13 \pm 0.06) \times 10^{-4}$	$(1.15 \pm 0.02) \times 10^{-3}$	$(1.83 \pm 0.03) \times 10^{-3}$
^{156}Eu	$(2.11 \pm 0.02) \times 10^{-4}$	$(6.37 \pm 0.06) \times 10^{-4}$	$(1.38 \pm 0.01) \times 10^{-3}$
^{161}Tb	$(2.40 \pm 0.13) \times 10^{-6}$	$(9.55 \pm 0.47) \times 10^{-6}$	$(6.58 \pm 0.07) \times 10^{-5}$

4. Measurement of ^{238}U (t,X) Cross Sections
(Decman, Estep, Henry, Mann, Meyer, Ussery)

We have bombarded a ^{238}U target with 16-MeV tritons, and have determined the production cross sections for a number of nearby nuclei. The target was a self-supporting uranium foil 1.6 mg/cm^2, irradiated in two stages: 0.4 nA triton beam for 90 h, immediately followed by a 225 nA beam for 2 h. The short-lived ^{237}Pa was counted in-beam during the low current bombardment. The long-lived radioactivities were counted off-line following irradiation. Because of time elapsed between the end of irradiation and the first count, only the sum of the cross sections for ^{239}U and ^{239}Np was determined. Detectors were calibrated using a ^{152}Eu calibration source. In a separate experiment, the fission cross section was estimated by counting both fission products and scattered tritons in a solid state detector at 98° relative to the beam direction. The program DWUCK was used to calculate the cross section for these scattered tritons, and thus by ratio, the fission cross section. The measured cross sections are summarized in Table A-3.

TABLE A-3. Cross section for fission and isotope production for ^{238}U + t.

Residual Nucleus	Cross Section (mb)	Residual Nucleus	Cross Section (mb)
^{237}Pa	12.8 ± 2.1	^{239}U + ^{239}Np	∿210
^{237}U	10.5 ± 1.8(a)	^{240}U	29 ± 3
^{238}Np	196 ± 21	^{240}Np	∿3
Fission	650		

(a) Virtually all of the ^{237}U comes from ^{237}Pa decay.

5. Neutron Capture Cross Sections for $^{86,87}Sr$ at Stellar Temperatures (Bauer, Becker, Howe, and Mathews)

Neutron capture cross sections for ^{86}Sr and ^{87}Sr have been measured for incident energies from 100 eV to 1 MeV at the Livermore electron linac using the white source of neutrons and time-of-flight techniques. The capture events were recorded by detecting the prompt gamma-ray cascade with two C_6D_6 scintillators, and were normalized to standard gold cross sections (see Fig. A-2). The neutron flux was monitored in a ^{6}Li-glass scintillator and the reliability of the background subtraction was checked with absorbers in the neutron beam. Corrections to the data were applied for neutron multiple scattering and self-shielding, gamma-ray absorption, and for detector response. The Maxwellian average neutron capture cross sections have been calculated for stellar temperatures ranging from kT = 10 to 100 keV. Capture rates for some representative temperatures are given in Table A-4.

The capture cross sections of the two pure shielded s-process nuclei ^{86}Sr and ^{87}Sr are of importance for stellar nucleosynthesis of nuclei in the mass region near the N = 50 closed shell. Specifically, they are important in the study of the s-process branching through ^{85}Kr as a monitor of the neutron capture time scale, and also in the investigation of the ^{87}Rb-^{87}Sr chronometric pair as an independent measure of the age of the galaxy.

TABLE A-4. Maxwellian averaged cross sections of the measured isotopes as a function of the thermal energy kT (preliminary values).

measured isotope	calculated Maxwellian averaged capture cross sections (mb) at 10 keV	30 keV	100 keV
^{86}Sr	115 ± 20	64 ± 10	35 ± 5
^{87}Sr	185 ± 20	98 ± 10	45 ± 5

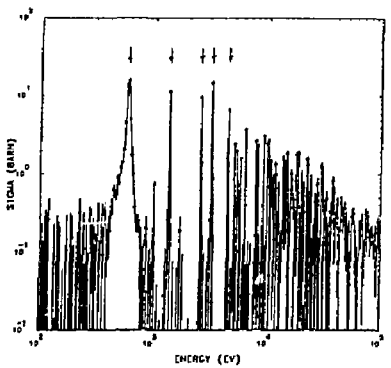

Fig. A-2. Measured capture cross section of ^{86}Sr, displaying strong resonances at 0.588, 1.370, 2.592, 3.247 and 4.496 keV.

6. Influence of Realistic Single Particle Spacings on Precompound Decay Spectra (Blann, Grimes,* Hansen, Komoto, Pohl, Scobel,** Trabandt,** and Wong)

We made (p,n) measurements on 3 targets[7] chosen to enhance the influence of single particle spacings on precompound decay spectra. These data are being interpreted in terms of one proton particle-one neutron hole residual state densities calculated with shell model single particle spacings rather than the more common equidistant spacing model. Nuclei involving the $g_{9/2}$ shell closure have been analyzed.[8] Nuclei involving the $f_{7/2}$ shell closure are presently being analyzed. In Fig. A-3 we show experimental angle integrated (p,n) spectra from $^{50,52,53}Cr$ targets compared with shell model based two-quasiparticle density calculations for spherical (Δ=0.00) and deformed (Δ=0.025) nuclei, using single particle energies due to Seeger-Howard[9] (S-H) and Seeger-Perisho[10] (S-P). The oscillator stiffnesses have been increased by 1/0.70, and BCS pairing strength of 0.75 MeV.

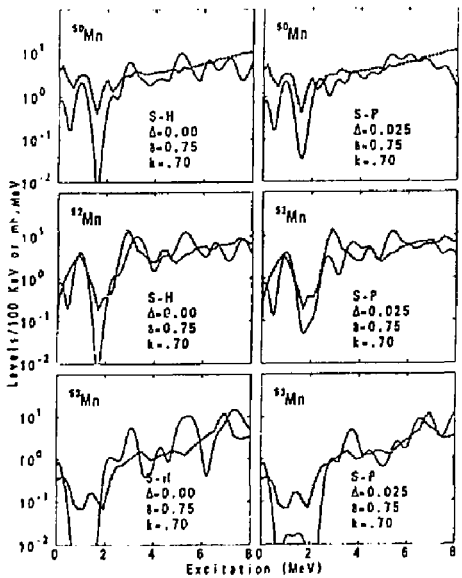

Fig. A-3. Experimental angle integrated (p,n) spectra from $^{50,52,53}Cr$ with 26 MeV incident protons, compared with (p) (n^{-1}) state densities calculated with realistic single particle levels. The connected open points represent the experimental spectra.

* Ohio University
** Hamburg University

7 W. Scobel, et al., LLNL Report No. UCID-20101 (1984) unpublished.
8 W. Scobel, et al., Phys. Rev. C30, 1480(1984).
9 P. A. Seeger and W. M. Howard, Nucl. Phys. A238, 491(1975).
10 P. A. Seeger and R. C. Perisho, LANL Report No. LA3751 (1967) unpublished.

7. Spontaneous Fissions from a Source of ^{260}Md
(Lougheed, Hulet, Wild, Dougan, Dupzyk, Henderson, Hahn)

We are measuring provisional mass and total kinetic energy (TKE) distributions of a spontaneous fission (SF) activity produced by bombarding a target of ^{254}Es with ^{18}O and ^{22}Ne ions. We collected recoiled transfer products from these bombardments on tantalum foils and transported them rapidly to an isotope separator. By isotope separation the fraction of mass 260 was collected on a thin aluminum foil and counted. This activity has a half-life of 30 ± 5 d and is believed to arise from previously unknown ^{260}Md, because all other isotopes of mass 260 are either known or are expected to have much shorter half-lives. Four possible sources of SF originate from this sample: direct SF decay of ^{260}Md, beta decay to short-lived ^{260}No, electron capture (EC) decay to very short-lived ^{260}Fm, and alpha decay leading to ^{256}Es and ^{256}Fm. The end products of the last three decay modes are SF emitters. One of our fission detectors also detects beta particles; when a SF event occurs, we record the times of occurrence of the five previous beta events in an effort to observe beta decay to ^{260}No. However, we have been unable to observe any difference between the interval from the last beta particle to the SF event and the intervals between the beta particle events, which are expected to be random. This suggests that beta decay is not a significant mode of decay of ^{260}Md. Figure A-4 shows the TKE and mass distributions we have obtained. The high-energy peak of the TKE distribution, centered at about 235 MeV, is associated with the narrow central peak of the mass distribution. It is possible that these high-energy SF events arise from the decay of ^{260}Fm, the EC-decay daughter, and are similar to those from the SF decay of ^{258}Fm and ^{259}Fm. We are continuing to analyze the decay of ^{260}Md.

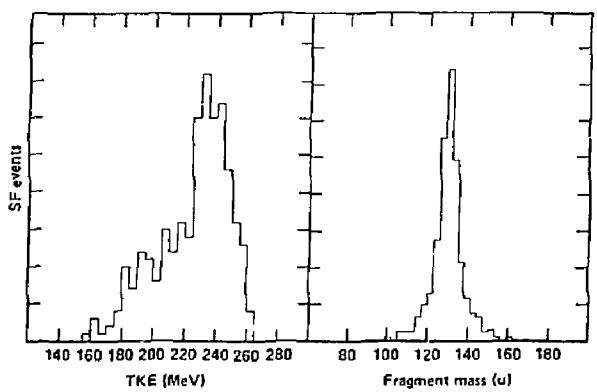

Fig. A-4. TKE and mass distributions. The data were obtained from ∿60 d of coincident fission-fragment counting.

8. Excitation Function Measurements from Proton and Deuteron Bombardment of Natural Ti (West and Lanier)

Excitation functions were measured by the activation method for the production of ^{48}V($\sim$16d) by protons and deuterons on targets of natural Ti. The measurements were made for a projectile energy range between $\sim$1.5 and 26 MeV (protons: $\sim$4.5 to 25 MeV; deuterons: $\sim$1.5 to 20 MeV). For measurements near threshold, the targets were thin 1 inch diameter evaporated deposits ($\sim$3.6 mg/cm^2) mounted on thick ($\sim$0.5 cm) aluminum disks. At higher energies, where the cross section is slowly varying, a series of foil stacks was irradiated. The stacks contained from 2 to 5, 1 inch diameter circular foils ($\sim$11 mg/cm^2) and each foil was separated by an appropriate thickness of aluminum degrader foil. Yields of ^{48}V were determined from the activated foils by γ-ray counting on well-calibrated (accuracy: ± 2%) Ge (Li) detector systems. To check the accuracy and reproducibility of our charge collection arrangement, we remeasured the well-known $^{65}Cu(p,n)$ cross section at several energies and found excellent agreement between our results and published values.[11] Allowing for unknown systematic errors, we believe that individual cross sections are accurate to ± 5%.

The results of our measurements are summarized in Fig. A-5. Although the targets were natural Ti, approximate individual excitation functions for the production of ^{48}V were obtained by dividing the raw data by the known isotopic abundances. The details are noted in the figure caption.[12] For future studies we plan complimentary measurements with isotopically enriched ^{47}, ^{48}, ^{49}Ti targets.

---

11 R. Colle, R. Kishore, and J. B. Cumming, Phys. Rev. C, 9, 1819 (1974).

12 Marshall Blann, private communication, statistical model code ALICE Lawrence Livermore National Laboratory, Livermore, CA, (1984).

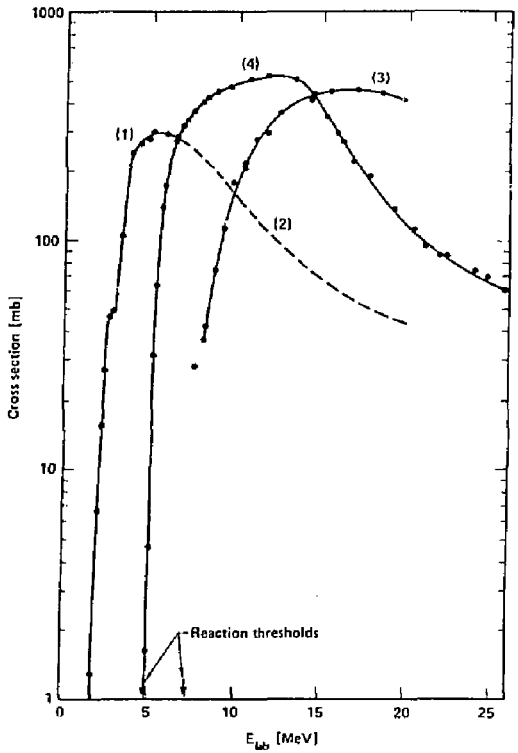

Fig. A-5. Excitation functions from p and d bombardment of natural Ti foils: (1) Ti (d,xn)^{48}V/0.0728 = ^{47}Ti(d,n)^{48}V, (2) extrapolated ^{47}Ti(d,n)^{48}V cross sections based on ALICE calculations, (3) Ti (d,xn) ^{48}V/0.7394 = ^{48}Ti(d,2n)^{48}V + contribution from ^{47}Ti, (4) Ti(p,xn)^{48}V/0.7394 = ^{48}Ti(p,n) ^{48}V + contribution from ^{49}Ti beginning at about 15 MeV.

B. NUCLEAR DATA APPLICATIONS - CALCULATIONS

1. Using Modeled Discrete Levels (Gardner, Gardner, and Hoff)

We have continued our study of isomer ratio calculations for the reactions: $^{175}Lu(n,\gamma)^{176m,g}Lu$, $^{175}Lu(n,2n)^{174,g}Lu$, $^{237}Np(n,2n)^{236m,g}Np$, $^{241}Am(n,\gamma)^{242m,g}Am$, and $^{243}Am(n,\gamma)^{244m,g}Am$. All of the cross-section calculations were made with our version of the STAPRE statistical model code,[1] with no fission competition. Below about 1.5 MeV in each deformed, odd-odd product nucleus, we replace the level density expression with a modeled discrete level set consisting of several hundred levels.[2]

The gamma-ray cascades leading to the ground-state and isomeric products are modeled as follows. The continuum bins are depopulated according to our E1 and M2 strength function systematics, where the E1 strength function has an energy-dependent Breit-Wigner line shape and the M2 strength function is a constant.[3] The depopulation of the discrete levels proceeds as described in Ref. 2. We have found that the use, among the discrete levels, of the same E1 and M1 strength functions as described for the continuum led to calculated isomer ratios for the $^{175}Lu(n,\gamma)$ and $^{237}Np(n,2n)$ reactions that were equal to those obtained using a constant E1/M1 ratio of 0.167.

The calculated g/m ratios for the $^{237}Np(n,2n)$ reaction are shown in Fig. B-1a, compared with a 14 MeV measurement.[4] Sensitivity studies of the computed isomer ratio relative to the number of discrete levels describing ^{236}Np also were made. Set A, consisting of 998 levels and 94 rotational bands, was truncated several times just below a new band head to yield Sets B-D. The distribution of the K quantum numbers, P(K), associated with Sets A-D are shown in Fig. B-1b. Although the P(K), of Sets A and B are different, each has a sufficiently representative sampling of K values to yield similar isomer ratios. Sets C and D do not sample all of the K values, leading to isomer ratios that are too high.

In Fig. B-2a we show our calculated m/g ratios for the $^{241}Am(n,\gamma)$ and $^{243}Am(n,\gamma)$ reactions compared with measurements.[5,6] We also computed isomer ratios for s-wave neutrons leading to the 2^- and 3^- resonances for comparison with the thermal and epithermal data. Other calculational results from Refs. 5 and 6 are shown too. For each reaction,

---

1 M. Uhl, Acta Phys. Austriaca 31, 241 (1970).
2 R. W Hoff, et al., "Level-Structure Modeling of Odd-Odd Deformed Nuclei," UCAR 10062-83/1 (1983), p. 218.
3 D. G. Gardner, ANL-83- (1983), p. 67.
4 W. A. Myers, et al., J. Inorg. Nucl. Chem. 37, 637 (1975).
5 K. Wisshak, et al., Nucl. Sci. Eng. 81, 396 (1982).
6 F. M. Mann and R. E. Schenter, Nucl. Sci. Eng. 63, 242 (1977).

our s-wave 3^- resonance result agrees well with data. Fission competition should not have a significant effect at thermal energies for target ^{241}Am and throughout the neutron energy range shown for target ^{243}Am. However, the lack of fission competition in our calculations may be the reason why our ^{241}Am isomer ratio is not in good agreement with the 30-keV data. For the $^{241}Am(n,\gamma)$ reaction, our isomer ratio for the 3^- resonance is larger than that for the 2^- resonance, in agreement with the Ref. 5 calculation. In Fig. B-2b we show the spin distributions among the discrete levels that we calculate after the gamma-ray cascade from the continuum for both the 2^- or 3^- resonance cases. These distributions show why the high spin state is favored by the 3^- resonance and why we obtain the relative order of the isomer ratios for each case.

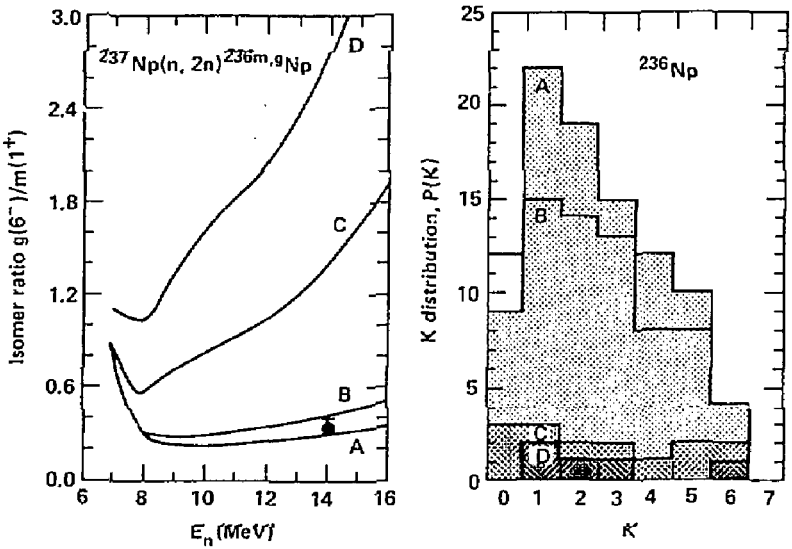

Fig. B-1 a) Calculated $^{237}Np(n,2n)$ *g/m ratios* vs E_n *using* ^{236}Np level Sets A-D, compared with data (●).[4] b) The P(K) for Sets A-D.

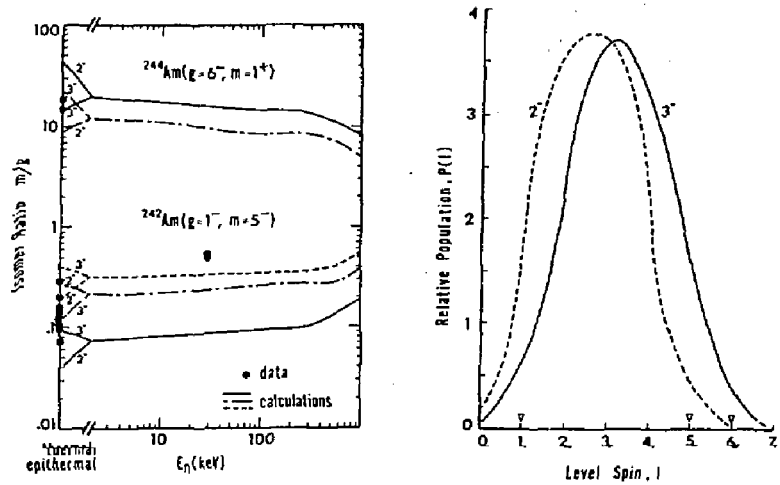

Fig. β-2 a) Calculated ^{241,243}Am (n,γ) n/g ratios vs E_n compared with data [5,6] (——— present work, ----- Ref. 5, - —— Ref. 6) b) Spin distributions among levels calculated after γ-ray cascade from continuum for 2$^-$ and 3$^-$ resonance cases.

2. Modeling Level Structures of Odd-Odd Deformed Nuclei
(Hoff, Kern, Piepenbring, and Boisson)

A technique for modeling quasiparticle excitation energies and rotational parameters in odd-odd deformed nuclei has been applied to actinide species where new experimental data have been obtained by use of neutron-capture gamma-ray spectroscopy. The input parameters required for the calculation were derived from empirical data on single-particle excitations in neighboring odd-mass nuclei. Calculated configuration-specific values for the Gallagher-Moszkowski splittings were used. Calculated and experimental level structures for ^{238}Np, ^{244}Am, and ^{250}Bk are compared, as well as those for several nuclei in the rare-earth region. The agreement for the actinide species is excellent, with bandhead energies deviating 22 keV and rotational parameters 5%, on the average. Corresponding average deviations for five rare-earth nuclei are 47 keV and 7%.

TABLE B-1. Odd-odd nuclei in actinide and rare-earth regions: Comparison of experimental and calculated bandhead energies (E), rotational parameters (A), and G-M splittings (E_{GM}).

Nucleus	Number of bands	Energy range (keV)	$\langle E_{exp}-E_{calc}\rangle$ (keV)	$\langle A_{exp}-A_{calc}\rangle$ (keV)	E_{GM} exp/calc
^{238}Np	9	0 - 345	29	0.14 (3.2%)	1.18,0.87
^{244}Am	16	0 - 680	19	0.28 (7.4%)	1.15,0.14,0.96
^{250}Bk	14	0 - 570	17	0.20 (4.7%)	1.11,0.96,2.87, 1.39,1.32
^{160}Tb	8	0 - 380	41	0.61 (8.1%)	1.03,1.07,1.13
^{166}Ho	10	0 - 560	47	0.74 (8.7%)	0.80,1.08,1.31
^{170}Tm	5	0 - 450	63	0.46 (5.2%)	2.04,0.98
^{176}Lu	12	0 - 840	58	1.0 (9.2%)	1.14,0.48,1.01, 0.91,0.39
^{182}Ta	7	0 - 270	24	0.47 (3.9%)	0.94,0.97,1.14

3. Test of a Phenomenological Model of Odd-Odd Deformed Nuclei: An ARC Study of ^{176}Lu (Hoff, Casten,* Bergoffen,* Warner*)

An average resonance capture (ARC) study leading to a complete set of $J^{\pi}=2^{-}-5^{-}$ levels in the odd-odd nucleus ^{176}Lu is reported. A phenomenological model for odd-odd nuclei, which is based on the empirical structure of the neighboring odd mass nuclei and which incorporates the effects of certain neutron-proton interactions, is utilized to interpret the data. Cumulative level-number histograms, obtained from this model, are in generally good agreement with the empirical results up to 1100 keV of excitation. The comparison involves a total of 40 predicted rotational bands (see Fig. B-3). Some specific discrepancies arise for 3^{-}, 4^{-} states in a model energy interval near E_x=700 keV, because of an anomalously large predicted Gallagher-Moszkowski splitting for the $1/2^{+}[411]p$; $7/2^{-}[514]n$ two-quasiparticle configuration and because of low predicted energies for states involving the $7/2^{+}[404]$ proton orbit.

* Brookhaven National Laboratory, Upton, NY 11973

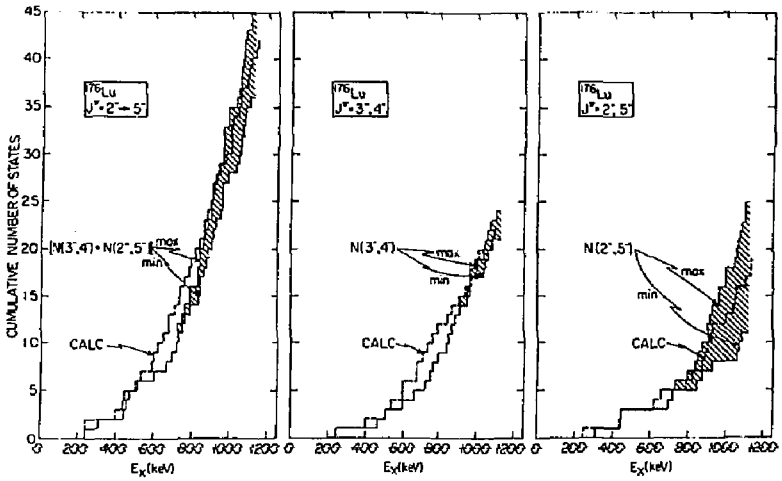

Fig. B-3. Cumulative level number histograms for all states in ^{176}Lu with spins $2^-,3^-,4^-,5^-$ (ieft), $3^-,4^-$ (middle) and $2^-,5^-$ (right). The cross hatched region shows the range of the maximum and minimum numbers of states allowed by the ARC data. The dashed lines show the results of the model calculations.

4. Absolute Dipole Gamma-ray Strength Functions for ^{176}Lu (Gardner, Gardner, Hoff)

We have derived absolute dipole strength-function information for ^{176}Lu from an average resonance capture study of ^{175}Lu with 2 keV neutrons and from neutron capture cross section measurements with neutrons from 30 keV to about 1 MeV. We found that we needed to increase our previous estimate of the relative M1/E1 strengths near 5 MeV by a factor of 3 and to revise downward the absolute magnitude of our E1 strength function. We accomplished the latter, while still maintaining continuity with the photonuclear data, by adjusting the one free parameter (E_x) in our line shape. The present E1 and M1 strengths now seem correct both near the neutron separation energy and also around 1 MeV.

In Fig. B-4 we show the newly derived E1 and M1 strength functions for ^{176}Lu, as a function of the γ-ray energy (the full curves). For comparison, we also show the results predicted by our original systematics[7] (the dashed curves) and from a Lorentz E1 strength function (the dotted curve). The arrows indicate the E_x value of 11 MeV determined in the present study and the 5 MeV value used previously.

In the E1 case, it is convenient to compare with experiment the function $S_{E1} = f_{E1}(E_\gamma)A^{-8/3}\,E_\gamma^{-2}$. The McCullagh et al.,[8] compilation of f_{E1} values expressed in this form is plotted in Fig. B-5. For ^{176}Lu at $E_\gamma = 5$ MeV, our new E1 strength function has a value of 5.1×10^{-8} MeV^{-3}, which converts to $S_{E1} = 2.1 \times 10^{15}$. The shaded rectangle in Fig. B-5 shows this value, along with the estimated error limits of ± 40%. The set of curves in the figure were predicted by our original systematics.

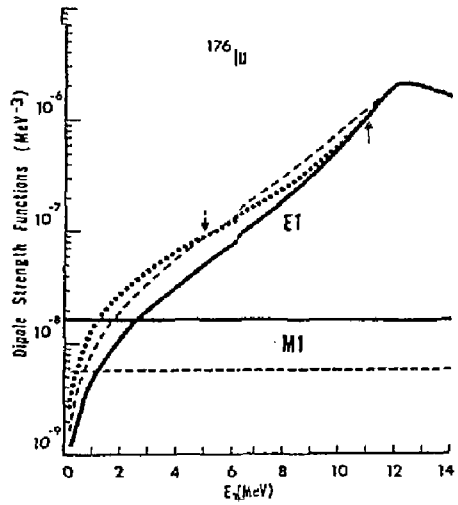

Fig. B-4. Absolute E1 and M1 strength functions for the ^{176}Lu nucleus.

---

7 D. G. Gardner, Proc. NEANDC/NEACRP Specialist's Meeting on Fast-Neutron Capture Cross Sections, Argonne, IL, ANL-83-4 (1983), p.67.

8 C. M. McCullagh, M. L. Stelts and R. E. Chrien, Phys. Rev. C23. 1394 (1981).

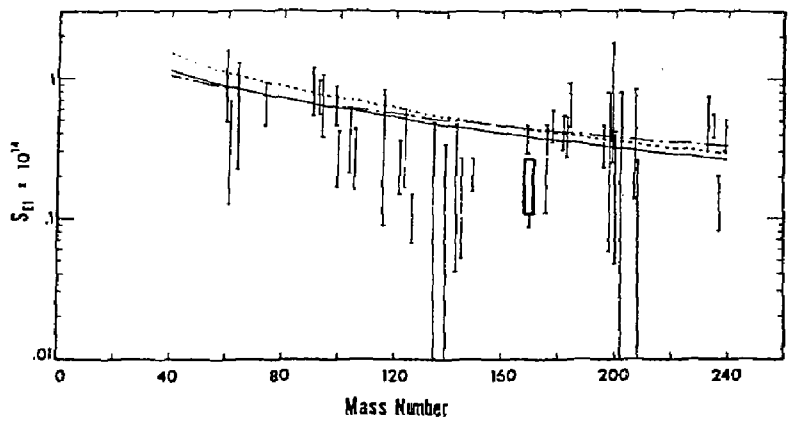

Fig. B-5. Comparison of E1 strength function value derived in this work for ^{176}Lu (shaded rectangle includes error estimate with the data from the compilation of McCullagh et al.[8] The curves are S_{E1} values predicted by our systematics[7] for γ-ray energies of 3, 5 and 7 MeV.

5. Gamow-Teller Matrix Elements from the $^{11}B(p,n)^{11}C$ Reaction at E_p = 26 MeV (Grimes,* Anderson, Davis, Howell, Wong, Carpenter,† Carr,† and Petrovich†)

The $^{11}B(p,n)^{11}C$ reaction has been investigated at 1 MeV intervals for proton bombarding energies in the E_p = 16-26 MeV range. In the experiment, final states in ^{11}C up to $E_x \approx 10$ MeV were clearly identified and differential cross sections were extracted for the first four levels in ^{11}C. The E_p = 26 MeV data are examined in microscopic DWA calculations using the wave functions of Cohen and Kurath[9] to describe the states in ^{11}B and ^{11}C and using the G matrix interaction of Bertsch et al.[10] for the effective nucleon-nucleon interaction. Gamow-Teller matrix elements for transitions to excited states in ^{11}C are extracted on the basis of these calculations, thus extending the information on GT matrix elements in the mass 11 systems beyond the ground state matrix element known from β-decay. Throughout, the results are contrasted with existing information from electromagnetic studies of ^{11}B.[11-13] It is concluded that the Cohen-Kurath model places too much GT strength in the low lying states of the mass 11 systems and not enough strength at higher excitation energies. In addition this model underestimates the net contribution to M1 matrix elements from the isoscalar spin and current and isovector current parts of the M1 operator. The extracted GT matrix elements for the first four levels in ^{11}C are in excellent agreement with those deduced from (p,n) measurements at E_p = 160 MeV.[14]

---

* Physics Dept., Ohio University, Athens, Ohio 45701

† Physics Dept., Florida State University, Tallahassee, Florida 32306

9 S. Cohen and D. Kurath, Nucl. Phys. 73, 1 (1965); A101, 1 (1967).

10 G. Bertsch et al., Nucl. Phys. A284, 399 (1977).

11 T. Stovall et al., Nucl. Phys. 86, 225 (1966).

12 R. E. Rand et al., Phys. Rev. 144, 859 (1966).

13 P. T. Kan et al., Phys. Rev. C11 323 (1975)

14 T. N. Taddeucci, private communication.

6. K-Distribution for Neutron Fission of ^{232}Th
(Becker and Bauer)

The ^{232}Th(n,f) fission fragment angular distributions have been measured for incident energies from 0.7 to 10 MeV using the white source of neutrons produced at the 100-MeV LLNL Electron Linear Accelerator Facility. Preliminary angular distribution data were presented in last year's report. In our recent analysis, the fragment angular distributions were binned in intervals of 40 keV, and fit using least-squares techniques to the following expression:

$$W(\Theta) = \sum_{K=\frac{1}{2},\frac{3}{2},\frac{5}{2}} A_K \sum_{J,\Pi} B^{\Pi}_{KJ} W_{KJ}(\Theta),$$

in order to obtain A_K, the distribution of K values among the transition states. The $W_{KJ}(\Theta)$ represent the weighted squared modulus of the wave-functions of the symmetric top, and the B^{Π}_{KJ} are obtained from a Hauser-Feshbach calculation of the partial fission cross-sections as described in Bjørnholm and Lynn.[15] The results for incident neutron energy $0.7 \leq E_n$ (MeV) ≤ 4.5 are presented in Fig. B-6.

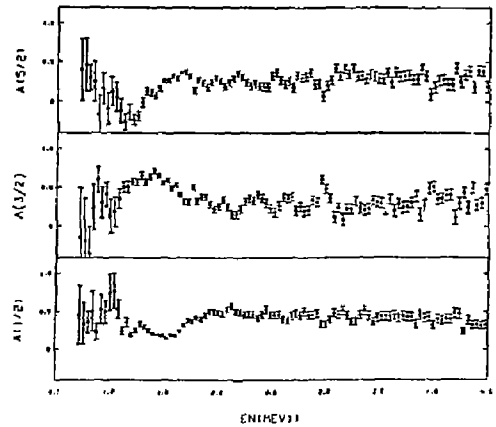

Fig. B-6. K-distribution in the transition nucleus ^{233}Th as a function of E_n. Note that for every E_n, $\sum_K A_K = 1.0$.

---

[15] S. Bjørnholm and J. E. Lynn, Rev. Mod. Phys. 52, 725 (1980).

7. A Shell Model Study of the $^{71}Ga(\nu,e^-)\,^{71}Ge$ Neutrino Detector (Mathews, Bloom, and Fuller*)

Gamow-Teller allowed neutrino-capture transitions between the ground-state of ^{71}Ga and accessible low-lying states in ^{71}Ge are calculated in a model space of the 2p and 1f shells. The total (p,n) Gamow-Teller strength function is also calculated (see Fig. B-7). The effects of model-space truncation are systematically investigated, and comparisons are made between calculated and experimental energies and spectroscopic factors for states in ^{71}Ga and ^{71}Ge as well as the E2 transition rate from the first excited state in ^{71}Ge. We find that the possible contributions to the count rate in a ^{71}Ga neutrino detector from transitions to excited states in ^{71}Ge are weaker than recent (p,n) measurements at 35 MeV seem to imply. However, these results, together with calculations of similar transitions in neighboring nuclei, indicate that the neutrino capture rate to the first excited state in ^{71}Ge is probably not as small as the value estimated on the basis of the systematics of similar transitions in this region.

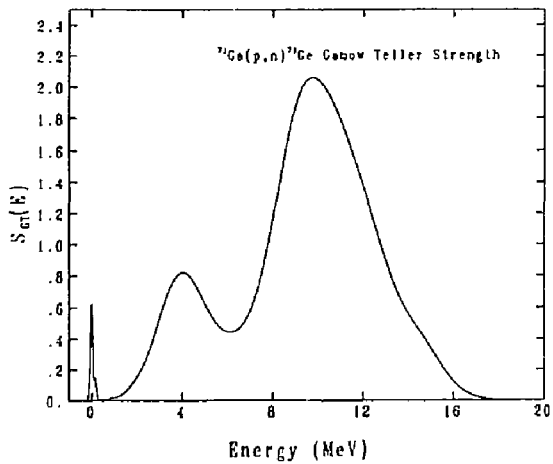

Fig. B-7. Gamow-Teller strength function for $^{71}Ga(p,n)^{71}Ge$.

* University of California, Santa Cruz

8. Extension of Microscopic Models for Neutron and Proton Scattering to Inelastic-Scattering and Charge-Exchange Reactions (Dietrich, Petrovich,* Finlay,** and Mellema**)

Results of a systematic study reported over the last two years have shown that a microscopic folding model yields reasonable results for elastic nucleon-scattering differential cross sections and neutron total cross sections in an energy range of roughly 7 to 50 MeV. The physical input to these calculations is the nuclear density and a complex, energy- and density-dependent effective interaction; we have tested three interactions derived from free nucleon-nucleon scattering via many-body theory.[16-18] The transition potentials for a number of other types of reactions, including inelastic scattering, (p,n) reactions to the isobaric-analog state, and radiative nucleon capture through giant multipole resonances, may be calculated in the same framework by replacing the nuclear density by the appropriate transition density. We have begun a study to determine whether a unified treatment of these reactions is successful, in which the same effective interaction is used for both the transition potentials and the distorting potentials for the incoming and outgoing waves.

A detailed summary of results obtained up to the present may be found in Ref. 19. Calculations have been made for the ^{208}Pb(p,n) isobaric-analog reaction, excitation of the first 2+ states in ^{54,56}Fe, and the first 3$^-$ states in ^{208}Pb and ^{16}O. It is found that damping of the scattering wave functions in the nuclear interior due to nonlocality (the Perey effect) is significant and can reduce cross sections by 20 to 30%. When this effect is taken into account, the results for inelastic scattering are reasonably well reproduced. Problems remain with the (p,n) charge exchange reaction, which may reflect a deficiency in the strength of the isovector part of the effective interaction; for example, the interaction based on Ref. 16 underestimates the ^{208}Pb(p,n) cross section by a factor of four, even though the shape of the angular distribution is acceptable.

---

* Florida State University, Tallahassee, FL 32306
** Ohio University, Athens, OH 45701

16 J. P. Jeukenne, A. Lejeune, and C. Mahaux, Phys. Rev. C16, 80 (1977).
17 F. A. Brieva and J. R. Rook, Nucl. Phys. A291, 299, 317 (1977).
18 N. Yamaguchi, S. Nagata, and T. Matsuda, Prog. Theor. Phys. (Japan) 70, 459 (1983).
19 F. S. Dietrich and F. Petrovich, in Neutron-Nucleus Collisions -- A Probe of Nuclear Structure, J. Rapaport et al., ed., AIP Conference Proceedings No. 124, p. 90 (1985).

C. NUCLEAR DATA APPLICATIONS - EVALUATIONS

1. A Reevaluation of the $^{9}Be(n,2n)$ Reaction (Perkins, Plechaty and Howerton)

Using a Monte Carlo technique and recent double-differential measurements, a new evaluation for the $^{9}Be(n,2n)$ reaction has been done. The secondary neutrons are represented as doubly-differential in angle and energy.

The new evaluation is currently being tested by comparison of calculated and experimental leakage spectra from 2.5 and 3.5 MFP ^{9}Be pulsed spheres as discussed elsewhere in this report. It has also been tested by calculating the multiplication constant (k_{eff}) for 16 just-critical assemblies, reflected by ^{9}Be with thicknesses ranging from 1.27 to 20.27 cm. In all cases the calculated k_{eff} value agreed with experiment within the calculational and experimental uncertainties.